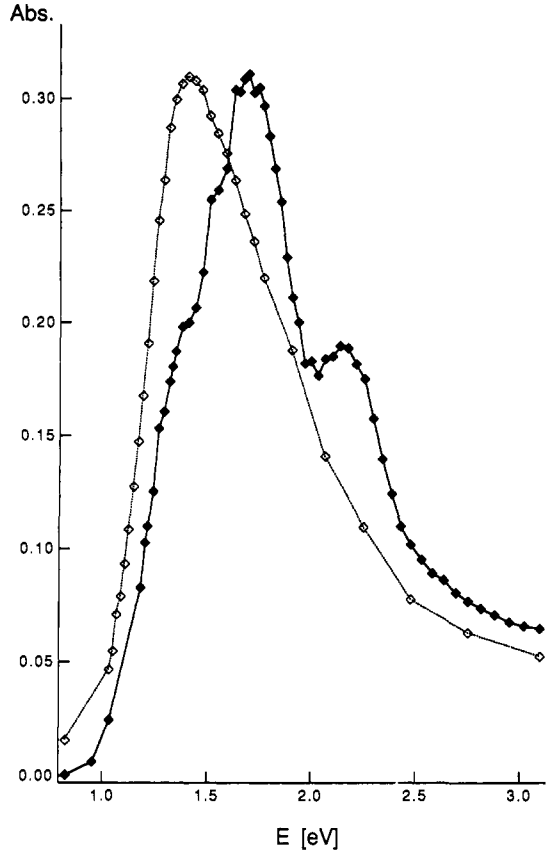

Figure 1. Room temperature spectra of (e^-,Na^+) in 2,5-DMTHF (solid line) and THF (dotted line). The scaling is arbitrary.

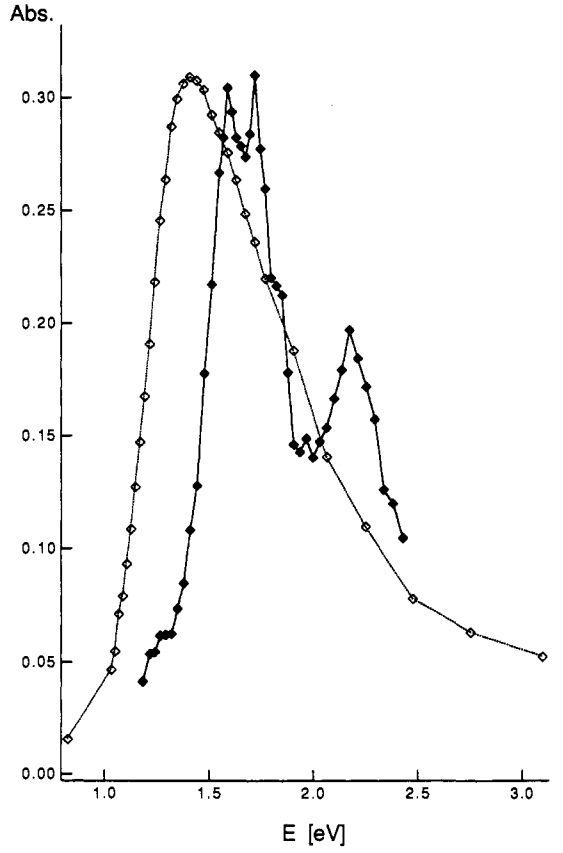

Figure 2. Room temperature spectra of (e^-,Na^+) in 2,5-TMTHF (solid line) and THF (dotted line). The scaling is arbitrary.

of Na^+ cations in the THF and 2,5-DMTHF measurements. Due to its insolubility in 2,5-TMTHF, the much more soluble tetrakis[3,5-bis(trifluoromethyl)phenyl]boron sodium was used instead. The experimental details will be published later.

The optical absorption spectrum of (e^-,Na^+) in 2,5-DMTHF consists of two clearly resolved peaks at 575 (2.15 eV) and 735 nm (1.69 eV) and a shoulder at longer wavelengths (Figure 1). The main peak is blue-shifted by 0.28 eV in comparison with the same salt in THF. There are three resolved peaks at 570 (2.17 eV), 720 (1.72 eV), and 780 nm (1.59 eV) in 2,5-TMTHF (Figure 2). The blue shift is not very different from the one in 2,5-DMTHF (the two highest peaks are shifted by 0.31 and 0.18 eV with respect to THF), but the spectral features are much sharper and the overall width of the spectrum is greatly reduced. While the possibility of a fast exchange between different sites remains open, the temporal behavior of the spectra down to approximately 1 ns supports the notion of a single chemical species (e^-,Na^+) being responsible for all the bands. Unfortunately, the assignment of the observed bands in terms of several bound → bound electronic transitions and one bound → continuum transition remains a nontrivial and ambiguous task, especially if (e^-,Na^+) is not spherically symmetric.

The results of the variable-temperature work, as well as measurements of electron attachment rates to various scavengers, will be presented in a more comprehensive article.

We will gladly make available the complete set of experimental data points to interested researchers.

Acknowledgment. We thank Mr. William Mulac for the excellent design of the collinear pulse radiolysis cell. We are indebted to Mr. George Cox and Mr. Donald Ficht for the consistent high quality of the LINAC beam.

Registry No. THF, 109-99-9; *cis*-2,5-DMTHF, 2144-41-4; *trans*-2,5-DMTHF, 2390-94-5; 2,5-TMTHF, 15045-43-9; Na^+, 17341-25-2.

Continuously Variable Hg–S Coordination in the Low-Dimensional Organic Metal (BEDT-TTF)$Hg_{0.776}(SCN)_2$ and Its Description by the Bond Valence Sum Method

Philip Coppens,* Ivana Cisarova,† Xianhui Bu, and Peter Sommer-Larsen‡

Chemistry Department
State University of New York at Buffalo
Buffalo, New York 14214

Received January 28, 1991

Composite crystals consist of two or more sublattices coexisting in the same crystal. The chemical composition of the crystal is therefore a function of the ratio of the sublattice volumes and is nonstoichiometric when the sublattices are incommensurate.[1] Examples are the organic superconductor (BEDT-TTF)$_4Hg_{2.89}Br_8$[2] and the metal (BEDO-TTF)$_{2.4}I_3$.[3] (BEDT-TTF = 3,4:3′,4′-bis(ethylenedithio)-2,2′,5,5′-tetrathiafulvalene, below referred to as ET; BEDO-TTF = 3,4:3′,4′-bis(ethylenedioxo)-2,2′,5,5′-tetrathiafulvalene.) The composite metal (ET)$Hg_{0.776}(SCN)_2$, synthesized by Wang et al.,[4] is particularly unusual as the Hg

* Author to whom correspondence should be addressed.
† Permanent address: Institute of Physics, Department of Structures and Bonding, Czechoslovakian Academy of Sciences, Na Slovance 2, 180 40 Praha 8, Czechoslovakia.
‡ Permanent address: Department for General Chemistry, The Royal Danish School of Pharmacy, DK-2100 Copenhagen, Denmark.

(1) Petricek, V.; Maly, K.; Coppens, P.; Bu, X.; Cisarova, I.; Frost-Jensen, A. *Acta Crystallogr.* **1991**, *A47*, 210–216.
(2) Lyubovskaya, R. N.; Zhilyaeva, E. I.; Petsoskii, S. I.; Lyubovskii, R. B.; Atovmyan, L. O.; D'yachenko, O. A.; Takhirov, T. G. *JETP Lett.* **1987**, *46*, 149–152.
(3) Cisarova, I.; Maly, K.; Bu, X.; Frost-Jensen, A.; Sommer-Larsen, P.; Coppens, P. *Chem. Mater.*, in press.

0002-7863/91/1513-5087$02.50/0

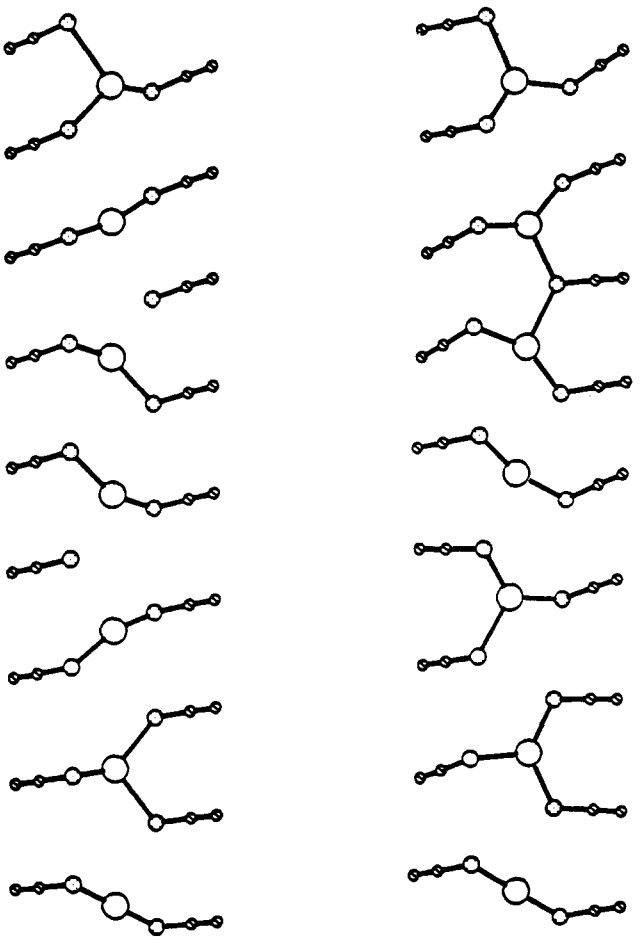

Figure 1. (a) Left: The coordination of Hg and SCN in the *average structure* of $(ET)Hg_{0.776}(SCN)_2$ as projected on the *ab* plane. The *b* axes of the two sublattices are vertical. The lack of commensurability leads to a continuously varying coordination. Connected atoms are at distances less than 3.0 Å. Large circles: Hg. Intermediate size circles: S. (b) Right: as at the left, *including the modulation.*

and SCN ions belong to different sublattices, even though the mercury ion is bonded to the S and (to a lesser extent) N atoms in its coordination sphere. We report here on the nature of the Hg–S coordination, which is continuously variable from unit cell to unit cell along the parallel, but incommensurate, *b* axes of the two sublattices, and on its analysis in terms of the valency of the mercury atoms.

The relation between the unit-cell edges of the two sublattices,[5] which each belong to the space group $P\bar{1}$, is described by the expression $A_{Hg} = \sigma A_{ET+SCN}$ with σ equal to

$$\begin{pmatrix} 1.0 & -0.0077 & 0 \\ 0 & 1.2903 & 0 \\ 0 & 0.9083 & 1 \end{pmatrix}$$

As shown in Figure 1a, in the *average* structure, in which the interaction between the sublattices is ignored, some of the SCN groups would not be coordinated, i.e., have Hg–S distances larger than 3.0 Å. In other unit cells, Hg–S distances are found that are, at 1.90 Å, much shorter than the Hg–S covalent coordination

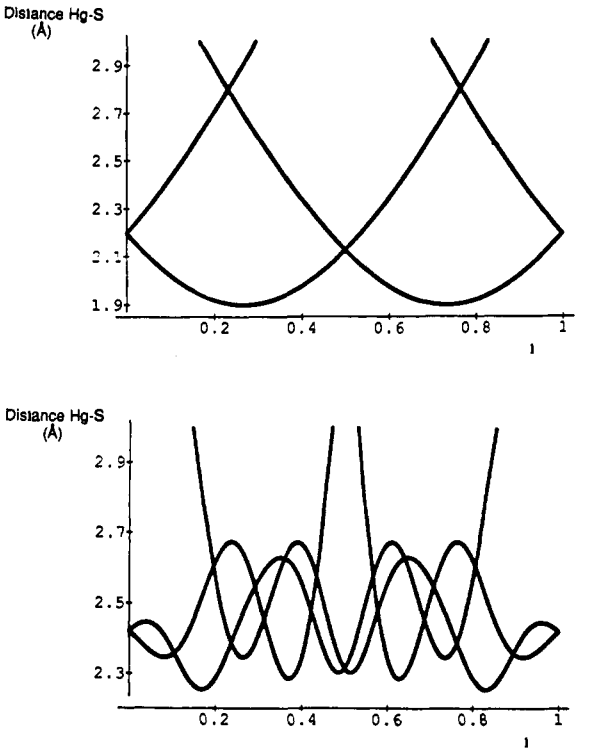

Figure 2. Hg–S distances as a function of the four-dimensional coordinate *t*. All Hg–S distances that occur in the crystal are represented in the figure. Top: for the average structure. Bottom: for the true structure including the modulation.

distance of about 2.30 Å.[6] This is an obviously unfavorable geometry. As a result, each of the sublattices is modulated with the periodicity of the second sublattice. The modulation is incommensurate because of the non-integer ratio of the *b*-axes lengths and gives rise to the occurrence of satellite reflections in the diffraction pattern. Analysis of the main and satellite reflections, as described elsewhere,[1] leads to the geometry shown in Figure 1b, in which all SCN ions are coordinated. The analysis is based on a four-dimensional description of the solid. In this method the fourth dimension is introduced such as to give a pattern periodic in four dimensions, even though, in three-dimensional, physical space, the translational symmetry in some directions is destroyed by the superposition of the incommensurate modulation. It is possible to plot all the distances that occur in the crystal as a function of the four-dimensional coordinate *t*, which is periodic in the interval $0 \leq t \leq 1$.[7] Any unit cell in the crystal can be associated with a particular value of *t*.[8] As shown in Figure 2, the anomalously short 1.90-Å Hg–S distance of the average structure is lengthened to 2.25 Å. On the other hand, the shortest Hg–N distance is reduced from 2.68 Å to 2.50 Å, indicating increased bonding to the N atoms, while the distance to the next-nearest sulfur atom is reduced from a maximum value of 2.80 Å to 2.60 Å.

The question may be asked to what extent the chemical bonding requirements have been satisfied by the modulations. To answer this question we have plotted the valence sums, as defined by Brown and Altermatt,[5] over all Hg–X contact distances to one

(4) Wang, H. H.; Beno, M. A.; Carlson, K. D.; Thorup, N.; Murray, A.; Porter, L. C.; Williams, J. M.; Maly, K.; Bu, X.; Petricek, V.; Cisarova, I.; Coppens, P.; Jung, D.; Whangbo, M.-H.; Schirber, J. E.; Overmyer, D. L. *Chem. Mater.*, in press.

(5) The BEDT-TTF donor molecule and SCN^- ligands form one subsystem with a triclinic cell ($P\bar{1}$, with dimensions $a = 6.746$ (2) Å, $b = 4.114$ (1) Å, $c = 20.580$ (3) Å, $\alpha = 83.06$ (1)°, $\beta = 105.93$ (2)°, $\gamma = 119.01$ (2)°, $V_{calcd} = 480.23$ Å^3, $Z = 1$) while the Hg atoms form a subsystem with a second triclinic cell ($P\bar{1}$, with dimensions $a = 6.758$ (2) Å, $b = 5.302$ (2) Å, $c = 21.352$ (6) Å, $\alpha = 73.10$ (2)°, $\beta = 110.44$ (3)°, $\gamma = 119.17$ (3)°, $V_{calcd} = 618.85$ Å^3, $Z = 1$).

(6) Brown, I. D.; Altermatt, D. *Acta Crystallogr.* **1985**, *B41*, 244–247.

(7) van Smaalen, S. *J. Phys.: Condens. Matter* **1991**, *3*, 1247–1263. Janner, A.; Janssen, T.; DeWolff, P. M. *Acta Crystallogr.* **1983**, *A39*, 671–678. Janner, A.; Janssen, T. *Acta Crystallogr.* **1980**, *A36*, 408–415.

(8) Two unit cells separated by a distance along the incommensurate direction correspond to different values of *t*. It can be shown that only atomic coordinates in one of the sublattices, and values of *t* in the interval $0 < t < 1$ to generate the positions in the second sublattice, are needed to obtain all existing interatomic distances between the two sublattices. The bond valence sum plotted in Figure 3 is summed over the coordination of the fully occupied Hg position. The coordination is a function of *t* because of the absence of the translational symmetry in the *b* direction in physical space. The treatment implicitly accounts for the nonstoichiometry of the overall structure.

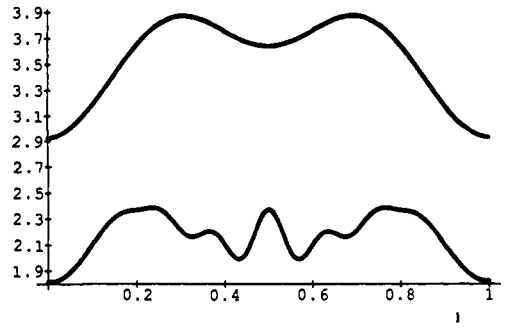

Figure 3. Valence sums for Hg as a function of the four-dimensional coordinate t. Top curve: for the average structure. Bottom curve: for the true structure including the modulation.

mercury atom as a function of the coordinate t. Figure 3 shows the results for both the average and the modulated structures. The Hg valence, which varies between 3.87 and 2.92 in the *average* structure, has, in the actual structure, much more reasonable values varying between 2.38 and 1.81, with a mean of 2.18. Thus the mercury atom has an average valency of close to 2, as may be expected, and a much smaller variation between unit cells than would have been the case in the absence of the modulation.

We conclude that the modulation in (BEDT-TTF)$Hg_{0.776}(SCN)_2$ is due to the coordination requirements of the central metal atom. The chemical nature of the modulation may be compared with modulations due to the lowering of the electronic energy in a valence band, such as occur in Peierls type metal–insulator transitions in low-dimensional solids. The continuous variation of the coordination, illustrated in Figure 1b, is highly unusual, but may become more common as additional complex solids are being synthesized.

Acknowledgment. This work was supported by the National Science Foundation (CHE8711736 and CHE9021069) and the donors of the Petroleum Research Fund, administered by the American Chemical Society (PRF21392-AC-6). We thank Dr. I. D. Brown of McMaster University for discussion of the valence sum method. The experimental results on which this analysis is based were obtained in collaboration with Drs. Wang, Beno, and Williams and co-workers at Argonne National Laboratory.

Enantioselective Synthesis of Mannostatin A: A New Glycoprotein Processing Inhibitor

S. Bruce King and Bruce Ganem*

Department of Chemistry, Baker Laboratory
Cornell University, Ithaca, New York 14853

Received March 15, 1991

The emergence of N-linked oligosaccharides on glycoproteins as important structural and functional domains in carbohydrate–protein interactions (e.g., recognition,[1] adhesion,[2] and transport[3]) is in large part due to the development of glycosidase inhibitors which have helped unravel the detailed trimming and processing events following glycosylation.[4] Until recently these naturally occurring inhibitors of glycoside hydrolysis were polyhydroxylated monocyclic[5,6] or bicyclic[7,8] alkaloids resembling either

Scheme I

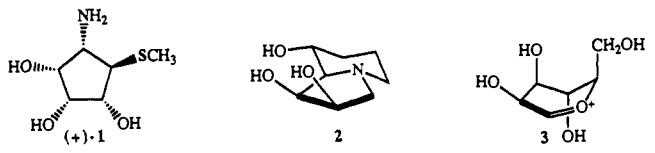

Scheme II

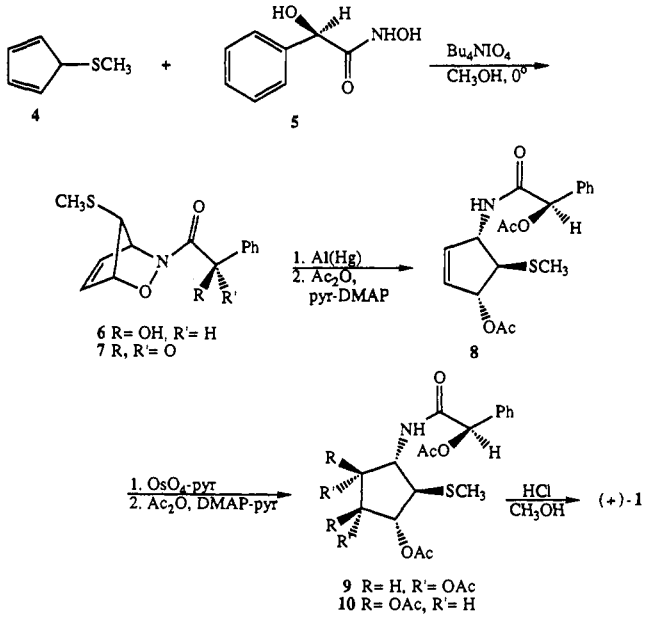

D-glucose or D-mannose.[9] However, in 1989 extracts of the soil microorganism *Streptoverticillium verticillus* were found to contain an unusual pentasubstituted cyclopentane **1** (Scheme I), which was named mannostatin A for its potent effect on rat epididymal α-mannosidase.[10] The structure and absolute stereochemistry of **1** shown in Scheme I were determined by X-ray diffraction.

Although its structure is quite different from the structures of known alkaloid-based inhibitors, compound **1** blocked Golgi processing mannosidase II more effectively than swainsonine (**2**) (IC_{50} = 200 nM;[8a] for **1**, 10–15 nM).[11] Such potent activity is all the more intriguing since mannostatin A bears little resemblance either to D-mannose or to the mannopyranosyl cation **3**, a putative hydrolysis intermediate.[12] Here we report a short, enantioselective total synthesis of **1** involving an unusual, syn-selective osmylation. Besides resolving certain questions surrounding the structure of **1**,[13] our work lays the groundwork for additional structure–activity studies of this remarkably potent new class of competitive glycosidase inhibitors.

(1) Sharon, N.; Lis, H. *Science* **1989**, *246*, 227.
(2) (a) Springer, T. A. *Nature* **1990**, *346*, 425. (b) Stoolman, L. M. *Cell* **1989**, *56*, 907.
(3) *Carbohydrate-Protein Interactions*; Clarke, A. E., Wilson, I. A., Eds.; Springer-Verlag: Heidelberg, 1988.
(4) Elbein, A. D. *Annu. Rev. Biochem.* **1987**, *56*, 497.
(5) 1-Deoxynojirimycin: Saunier, B.; Kilker, R. P.; Tkacz, J. S.; Quaroni, A.; Herskovics, A. *J. Biol. Chem.* **1982**, *257*, 14155.
(6) 1-Deoxymannojirimycin: (a) Fuhrmann, U.; Bause, E.; Legler, G.; Ploegh, H. *Nature* **1984**, *307*, 755. (b) Elbein, A. D.; Legler, G.; Tlusty, A.; McDowell, W.; Schwartz, R. T. *Arch. Biochem. Biophys.* **1984**, *235*, 579.
(7) Castanospermine: Pan, Y. T.; Hori, H.; Saul, R.; Sanford, B. A.; Molyneux, R. J.; Elbein, A. D. *Biochemistry* **1983**, *22*, 3975.
(8) Swainsonine: (a) Tulsiani, D. P. R.; Harris, T. M.; Touster, O. *J. Biol. Chem.* **1982**, *257*, 7936. (b) Elbein, A. D.; Solf, R.; Dorling, P. R.; Vosbeck, K. *Proc. Natl. Acad. Sci. U.S.A.* **1981**, *78*, 7393.
(9) Current review: Legler, G. *Adv. Carbohydr. Chem. Biochem.* **1990**, *48*, 319.
(10) (a) Aoyagi, T.; Yamamoto, T.; Kojiri, K.; Morishima, H.; Nagai, M.; Hamada, M.; Takeuchi, T.; Umezawa, H. *J. Antibiot.* **1989**, *42*, 883. (b) Morishima, H.; Kojiri, K.; Yamamoto, T.; Aoyagi, T.; Nakamura, H.; Iitaka, Y. *J. Antibiot.* **1989**, *42*, 1008.
(11) Tropea, J. E.; Kaushal, G. P.; Pastuszak, I.; Mitchell, M.; Aoyagi, T.; Molyneux, R. J.; Elbein, A. D. *Biochemistry* **1990**, *29*, 10062.
(12) Winkler, D. A.; Holan, G. *J. Med. Chem.* **1989**, *32*, 2084.
(13) Several structural details were of concern, notably the unusually deshielded ^1H NMR chemical shifts in **1** (e.g., S–CH_3 at 2.66 ppm), the absence of specific rotation data, and the fact that the enantiomer of the published structure more closely resembles the transition state for mannopyranoside hydrolysis.

0002-7863/91/1513-5089$02.50/0